Hindawi
Mathematical Problems in Engineering
Volume 2019, Article ID 6528251, 11 pages
https://doi.org/10.1155/2019/6528251

Research Article

Dynamic Analysis of Cracked Plate Subjected to Moving Oscillator by Finite Element Method

Nguyen Thai Chung,[1] **Nguyen Thi Hong**,[2] **and Le Xuan Thuy**[1]

[1] *Department of Solid Mechanics, Le Quy Don Technical University, Ha Noi, Vietnam*
[2] *Thuyloi University, Ha Noi, Vietnam*

Correspondence should be addressed to Nguyen Thai Chung; chungnt@mta.edu.vn

Received 4 April 2019; Revised 8 June 2019; Accepted 3 July 2019; Published 25 July 2019

Academic Editor: Arkadiusz Zak

This paper presents the finite element algorithm and results of dynamical analysis of cracked plate subjected to moving oscillator with a constant velocity and any motion orbit. There are many surveys considering the dynamic response of the plate when there is a change in number of cracks and the stiffness of the spring k. The numerical survey results show that the effect of cracks on the plate's vibration is significant. The results of this article can be used as a reference for calculating and designing traffic structures such as road surface and bridge surface panels.

1. Introduction

There are several types of plate structures affected by the vehicle load: pavement, railway system, and bridge floor, etc. Calculating these types of structures and the means of loading are modeled by different kinds of forces such as force, mass, and moving oscillators. Typically, the tracked vehicle is a moving mass, while the wheeled vehicle is described as a moving oscillator. Accordingly, structural dynamic analysis under the influence of mobile loads has been considered by many scientists. Nguyen Thai Chung and Le Pham Binh [1] analyzed the cracked beam on the elastic foundation under moving mass by using the finite element method (FEM). S.R. Mohebpour and P. Malekzadeh [2], P. Malekzadeh, A.R. Fiouz, H. Razi [3], Qinghua Song, Zhanqiang Liu, Jiahao Shi, Yi Wan [4], Qinghua Song, Jiahao Shi, and Zhanqiang Liu [5] presented a finite element model based on the first order shear deformation theory to investigate the dynamic behavior of laminated composite, FGM plates traversed by a moving oscillator, and a moving mass. Ahmad Mamandi, Ruhollah Mohsenzadeh, and Mohammad H. Kargarnovin [6] used finite element methods and Ansys software to simulate the nonlinear dynamic of rectangular plates subjected to accelerated or decelerated moving load. A.R. Vosoughi, P. Malekzadeh, and H. Razi [7] analyzed the moderately thick laminated composite plates on the elastic foundation subjected to moving load. G.L. Oian, S.N. Gu, J.S. Jiang [8], and Marek Krawczuk [9] analyzed the cracked plate subjected to dynamic loads by FEM. Yin T. and Lam H.F [10, 11] used a new solution method for investigation of the vibration characteristics of finite-length circular cylindrical shells with a circumferential part-through crack with four representative sets of boundary conditions being considered: simply supported, clamped-clamped, clamped-simply supported, and clamped-free. Li D. H., Yang X., Qian R. L., and Xu D. [12, 13] used the extended layer method (XLWM) to analyze the static reaction, free vibration, and transient response of cracked FGM plates.

2. Finite Element Simulation and Dominant Equations

Figure 1 shows the cracked plate under the moving oscillator on the plate in the general coordinate system (X,Y,Z).

For finite element model formulation, the following assumptions are made:

(i) The materials of the system are linear elastic.

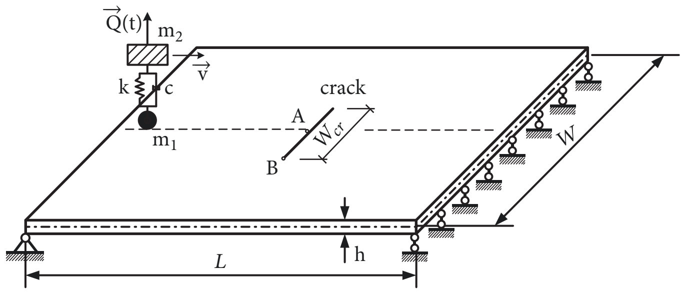

Figure 1: Cracked plate subjected to moving oscillator.

(ii) The load and pavement are not speared in the activity duration of system.

2.1. Cracked Plate Element Subjected to Moving Oscillator

2.1.1. Cracked Plate Element Subjected to Dynamic Loads. Plate is described by bending rectangular four-node elements (Figure 2). Arbitrary point in the element has positions (x, y) in global coordinate and positions (r, s) in local coordinate [14]. We assume that the thickness of plate element h is a constant and the conditions of Mindlin–Reissner plate theory are satisfied.

The displacement fields are written as [15]

$$\begin{aligned} u(x,y,z,t) &= u_0(x,y,t) + z\theta_y(x,y,t), \\ v(x,y,z,t) &= v_0(x,y,t) - z\theta_x(x,y,t), \\ w(x,y,z,t) &= w_0(x,y,t), \end{aligned} \tag{1}$$

where u_0, v_0, w_0 are the displacements of the mid plane and θ_x, θ_y are rotations of normal about, respectively, the y and x axes.

The strain vector is presented in the form

$$\{\varepsilon_p\} = \{\{\varepsilon_x \;\; \varepsilon_y \;\; \gamma_{xy}\} \;\; \{\gamma_{xz} \;\; \gamma_{yz}\}\}^T = \left\{\{\varepsilon^b\}^T \;\; \{\varepsilon^s\}^T\right\}^T, \tag{2}$$

where

$$\begin{aligned} \{\varepsilon^b\} &= \left\{\frac{\partial u_0}{\partial x} \;\; \frac{\partial v_0}{\partial y} \;\; \left(\frac{\partial u_0}{\partial y} + \frac{\partial v_0}{\partial x}\right)\right\}^T \\ &\quad + z\left\{\frac{\partial \theta_y}{\partial x} \;\; -\frac{\partial \theta_x}{\partial y} \;\; \left(\frac{\partial \theta_y}{\partial x} - \frac{\partial \theta_x}{\partial y}\right)\right\}^T \\ &= \{\varepsilon_0\} + z\{\kappa\}, \end{aligned} \tag{3}$$

$$\{\varepsilon^s\} = \{\gamma_{xz} \;\; \gamma_{yz}\}^T = \left\{\frac{\partial w_0}{\partial x} + \theta_y \;\; \frac{\partial w_0}{\partial y} - \theta_x\right\}^T, \tag{4}$$

$$\begin{aligned} \{\kappa\} &= \{k_x \;\; k_y \;\; k_{xy}\}^T \\ &= \left\{\frac{\partial \theta_y}{\partial x} \;\; -\frac{\partial \theta_x}{\partial y} \;\; \left(\frac{\partial \theta_y}{\partial x} - \frac{\partial \theta_x}{\partial y}\right)\right\}^T. \end{aligned} \tag{5}$$

The constitutive equation can be written as

$$\{\sigma\} = \left\{\begin{matrix}\{\sigma^b\} \\ \{\sigma^s\}\end{matrix}\right\} = \left[\begin{array}{c|c}[D^b] & [0] \\ \hline [0] & [D^s]\end{array}\right] \left\{\begin{matrix}\{\varepsilon^b\} \\ \{\gamma^s\}\end{matrix}\right\}, \tag{6}$$

where $\{\sigma^b\}$ is stress vector without shear deformation:

$$\begin{aligned} \{\sigma^b\} &= \begin{Bmatrix}\sigma_x \\ \sigma_y \\ \tau_{xy}\end{Bmatrix} = \frac{E}{1-\nu^2}\begin{bmatrix}1 & \nu & 0 \\ \nu & 1 & 0 \\ 0 & 0 & \dfrac{1-\nu}{2}\end{bmatrix}\begin{Bmatrix}\varepsilon_x \\ \varepsilon_y \\ \gamma_{xy}\end{Bmatrix} \\ &= [D^b]\{\varepsilon^b\} = [D^b](\{\varepsilon_0\} + z\{\kappa\}), \end{aligned} \tag{7}$$

$\{\sigma^s\}$ is stress vector of shear stress:

$$\begin{aligned} \{\sigma^s\} &= \begin{Bmatrix}\tau_{xz} \\ \tau_{yz}\end{Bmatrix} = G\begin{Bmatrix}\gamma_{xz} \\ \gamma_{yz}\end{Bmatrix} = \frac{E}{2(1+\nu)}\begin{bmatrix}1 & 0 \\ 0 & 1\end{bmatrix}\begin{Bmatrix}\gamma_{xz} \\ \gamma_{yz}\end{Bmatrix} \\ &= [D^s]\{\varepsilon^s\}, \end{aligned} \tag{8}$$

with E being elastic modulus of longitudinal deformation and ν being Poisson ratio.

Using (7) and (8), the components of internal force vector $\{F^{if}\}$ are determined as

$$\begin{aligned} \{M_x \;\; M_y \;\; M_{xy}\}^T &= \int_{-h/2}^{h/2} z \begin{Bmatrix}\sigma_x \\ \sigma_y \\ \tau_{xy}\end{Bmatrix} dz \\ &= [D^b]\int_{-h/2}^{h/2} z(\{\varepsilon_0\} + z\{\kappa\})\,dz \\ &= \frac{h^3}{12}[D^b]\{\kappa\}, \\ \{Q_x \;\; Q_y\}^T &= \int_{-h/2}^{h/2}[D^s]\{\varepsilon^s\}\,dz = \alpha h[D^s]\{\varepsilon^s\}, \end{aligned} \tag{9}$$

so that one obtains

$$\{F^{if}\} = [D^{cs}]\{\varepsilon^{cs}\}, \tag{10}$$

where $[D^{cs}] = \left[\begin{array}{c|c}(h^3/12)[D^b] & [0] \\ \hline [0] & \alpha h[D^s]\end{array}\right]$- strain matrix, $\{\varepsilon^{cs}\} = \{k_x \;\; k_y \;\; k_{xy} \;\; \gamma_{xz} \;\; \gamma_{yz}\}^T$ is the vector of curvatures

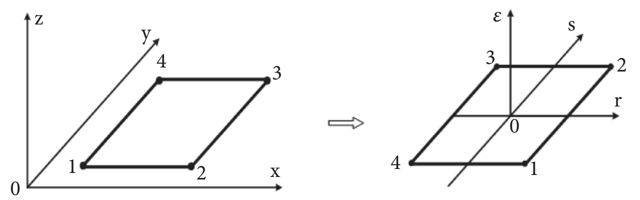

(a) In the general coordinate system (b) In the natural coordinate system

Figure 2: Model of 4-node plate element and the coordinate system.

and shear strains, and α is the shear strain correction factor, usually equal to $\alpha = 5/6$.

According to the FEM procedure, the displacement of a point of the element is represented as [14, 16]

$$w = \sum_{i=1}^{4} N_i w_i, \quad \theta_x = \sum_{i=1}^{4} N_i \theta_{xi}, \quad \theta_y = \sum_{i=1}^{4} N_i \theta_{yi}, \tag{11}$$

where w_i, θ_{xi}, θ_{yi} are displacements w, θ_x, θ_y at i^{th} node, respectively, and N_i are shape functions, which allows us to obtain

$$\{\varepsilon^{cs}\}_e = [B]\{q\}_e = \sum_{i=1}^{4} [B_i]\{q_i\}, \tag{12}$$

where $[B]_e$ is a matrix for the internal force determination, and $\{q\}_e = \left\{\{q_1\}^T \ \{q_2\}^T \ \{q_3\}^T \ \{q_4\}^T\right\}_e^T$ is a vector of the node displacement, with $\{q_i\} = \{w_i \ \theta_{xi} \ \theta_{yi}\}^T$, (i = 1,2,3,4).

Substituting (12) into (10) leads to

$$\left\{F^{if}\right\} = \sum_{i=1}^{4} [D^{cs}B_i]\{q_i\}, \tag{13}$$

$$\text{where } [D^{cs}B_i] = [D^{cs}B_i]^b + [D^{cs}B_i]^s, \tag{14}$$

$[D^{cs}B_i]^b$, $[D^{cs}B_i]^s$ are matrices corresponding to bending moment and shear force, respectively, [10, 11].

The dynamic equation of plate element can be derived by using Hamilton's principle [14, 17]:

$$\delta \int_{t_1}^{t_2} [T_e - \Pi_e]\, dt = 0, \tag{15}$$

where T_e, Π_e are kinetic energy and total potential energy of the element, respectively.

The kinetic energy of the element level is defined as [14]

$$\begin{aligned} \Pi_e &= \frac{1}{2}\int_{A_e} \left\{F^{if}\right\}_e^T [D^{cs}] \left\{F^{if}\right\}_e dA_e - \int_{A_e} wp dA_e \\ &= \frac{1}{2}\{q\}_e^T [K_0]_e \{q\}_e - \{q\}_e^T \{f\}_e, \end{aligned} \tag{16}$$

with $[K_0]_e = \int_{A_e}[B]^T[D^{cs}][B]dA_e$, $\{f\}_e = \int_{A_e}[N]^T p dA_e$ being stiffness matrix and node loading vector of the element, respectively, [N] is mode shape function matrix of element, p is pressure of intensity, $w = [N]\{q\}_e$, and A_e is the surface area of the plate elements.

Kinetic energy T_e of element is determined by [14]

$$\begin{aligned} T_e &= \frac{1}{2}\int_{V_e} \rho \{\dot{u}\}_e^T \{\dot{u}\}_e dV_e \\ &= \frac{1}{2}\{\dot{q}\}_e^T \left(\int_{V_e} \rho [N]^T [N]\, dV_e\right)\{\dot{q}\}_e \\ &= \frac{1}{2}\{\dot{q}\}_e^T [M_0]_e \{\dot{q}\}_e, \end{aligned} \tag{17}$$

where $[M_0]_e = \int_{V_e} \rho [N]^T [N] dV_e$ - mass matrix, ρ - mass density and $\{\dot{q}\}_e$-velocity vector.

Substituting (16) and (17) into (15), the dynamic matrix equation of the plate element without damping can be written as

$$[M_0]_e \{\ddot{q}\}_e + [K_0]_e \{q\}_e = \{f\}_e. \tag{18}$$

In the case of cracked plate element, the stiffness matrix $[K_c]_e$ of the element can be written as [8, 18]

$$[K_c]_e = [T]^T \left[C_f\right]^{-1} [T], \tag{19}$$

where [T] is the transformation matrix, given in Appendix A, $[C^f] = [C_0^f] + [C_1^f]$ in which $[C_0^f]$ is the flexibility matrix of the noncracked element, given in Appendix B, and $[C_1^f]$ is the flexibility matrix due to the presence of the crack, given in Appendix C [8].

Now, the dynamic matrix equations of the cracked plate element subjected to dynamic loads become

$$[M_0]_e \{\ddot{q}\}_e + [K_c]_e \{q\}_e = \{f\}_e. \tag{20}$$

2.1.2. Cracked Plate Element Subjected to Moving Oscillator. The force of the moving oscillator on the plate at the time t is determined as follows:

$$R(t) = \left(-m_1 \frac{d^2 w(x,y,t)}{dt^2} - m_2 \ddot{u} - (m_1 + m_2) g + Q(t)\right)\Bigg|_{\substack{x=\xi \\ y=\eta}}, \tag{21}$$

where g is acceleration due to gravity, $\ddot{u}$ is acceleration of the mass m_2, and $d^2w(x, y, t)/dt^2 = \ddot{w}$ is acceleration of the plate at the force set point given by

$$\frac{d^2w}{dt^2} = \left(\frac{\partial^2 w}{\partial x^2}\dot{x}^2 + \frac{\partial^2 w}{\partial y^2}\dot{y}^2 + \frac{\partial^2 w}{\partial t^2} + 2\frac{\partial^2 w}{\partial x \partial y}\dot{x}\dot{y} + 2\dot{x}\frac{\partial^2 w}{\partial x \partial t} + 2\dot{y}\frac{\partial^2 w}{\partial y \partial t} + \ddot{x}\frac{\partial w}{\partial x} + \ddot{y}\frac{\partial w}{\partial y}\right). \tag{22}$$

Substituting $w = [N]\{q\}_e$ into (22) yields

$$\frac{d^2w}{dt^2} = \left([N_{xx}]\dot{x}^2\{q\}_e + [N_{yy}]\dot{y}^2\{q\}_e + [N]\{\ddot{q}\}_e + 2\dot{x}\dot{y}[N_{xy}]\{q\}_e + 2\dot{x}[N_x]\{\dot{q}\}_e + 2\dot{y}[N_y]\{\dot{q}\}_e + \ddot{x}[N_x]\{q\}_e + \ddot{y}[N_y]\{q\}_e\right), \tag{23}$$

where $[N_x] = \partial[N]/\partial x$, $[N_{xx}] = \partial^2[N]/\partial x^2$, $[N_{xy}] = \partial^2[N]/\partial x\partial y$, $[N_y] = \partial[N]/\partial y$, $[N_{yy}] = \partial^2[N]/\partial y^2$, $\dot{x}, \dot{y}$ and $\ddot{x}, \ddot{y}$ are the velocity and acceleration of the loads along x, y axes, respectively.

By substituting (23) into (22), the force of the moving oscillator on the plate at the time t can be written as

$$R(t) = Q(t) - m_1[N]\{\ddot{q}\}_e - 2m_1\left(\dot{x}[N_x] + \dot{y}[N_y]\right) \cdot \{\dot{q}\}_e - m_1\left([N_{xx}]\dot{x}^2 + [N_{yy}]\dot{y}^2 + 2\dot{x}\dot{y}[N_{xy}] + \ddot{x}[N_x] + \ddot{y}[N_y]\right)\{q\}_e - m_2\ddot{u} - (m_1 + m_2)g. \tag{24}$$

Concentrated force (24) is described by the uniformly distributed load as follows [12–14]:

$$p(x, y, t) = \delta(x - \xi)\delta(y - \eta)R(x, y, t), \tag{25}$$

where $\delta(.)$ is the Dirac's delta function, and

$$\int_{-\infty}^{\infty} \delta(x - a) f(x)\,dx = f(a), \tag{26}$$

$$\int_a^b \delta(x - \xi) f(x)\,dx = \begin{cases} 0 & \text{if } \xi < a < b \\ f(\xi) & \text{if } a < \xi < b \\ 0 & \text{if } a < b < \xi. \end{cases} \tag{27}$$

Substituting (24) into (25) leads to

$$p = Q\delta(x - \xi)\delta(y - \eta) - m_1[N]\delta(x - \xi)\delta(y - \eta) \cdot \{\ddot{q}\}_e - 2m_1\left(\dot{x}[N_x] + \dot{y}[N_y]\right)\delta(x - \xi)\delta(y - \eta) \cdot \{\dot{q}\}_e - m_1\begin{pmatrix}[N_{xx}]\dot{x}^2 + [N_{yy}]\dot{y}^2 + 2\dot{x}\dot{y}[N_{xy}] + \\ +\ddot{x}[N_x] + \ddot{y}[N_y]\end{pmatrix}\delta(x - \xi)\delta(y - \eta)\{q\}_e - m_2\ddot{u}\delta(x - \xi)\delta(y - \eta) - (m_1 + m_2)g\delta(x - \xi)\delta(y - \eta). \tag{28}$$

The element nodal load vector is [14]

$$\{f\}_e = \int_0^b \int_0^a [N]^T p(x, y, t)\,dxdy = \int_0^b \int_0^a [N]^T \delta(x - \xi)\delta(y - \eta)R(x, y, t)\,dxdy. \tag{29}$$

Substituting (28) into (29) leads to the nodal load vector equation

$$\{f\}_e = \{P\}_e - \left[M_p^{m_1}\right]_e\{\ddot{q}\}_e - \left[M_p^{m_2}\right]_e\ddot{u} - \left[C_p\right]_e\{\dot{q}\}_e - \left[K_p\right]_e\{q\}_e, \tag{30}$$

where

$$\{P(t)\}_e = [N(\xi, \eta)]^T(Q - (m_1 + m_2)g), \tag{31}$$

$$\left[M_p^{m_1}\right]_e = m_1[N(\xi, \eta)]^T[N(\xi, \eta)], \tag{32}$$

$$\left[M_p^{m_2}\right]_e = m_2[N(\xi, \eta)]^T, \tag{33}$$

$$\left[C_p\right]_e = 2m_1[N(\xi, \eta)]^T\left(\dot{x}[N_x(\xi, \eta)] + \dot{y}[N_y(\xi, \eta)]\right), \tag{34}$$

$$\left[K_p\right]_e = m_1[N(\xi, \eta)]^T\left([N_{xx}(\xi, \eta)]\dot{x}^2 + [N_{yy}(\xi, \eta)]\dot{y}^2 + 2\dot{x}\dot{y}[N_{xy}(\xi, \eta)] + \ddot{x}[N_x(\xi, \eta)] + \ddot{y}[N_y(\xi, \eta)]\right), \tag{35}$$

Substituting (30) into (20) leads to the dynamic equation of the cracked plate element subjected to moving oscillator, which is

$$\left([M_0]_e + \left[M_p^{m_1}\right]_e\right)\{\ddot{q}\}_e + \left[M_p^{m_2}\right]_e\ddot{u} + \left[C_p\right]_e\{\dot{q}\}_e + \left([K_c]_e + \left[K_p\right]_e\right)\{q\}_e = \{P\}_e. \tag{36}$$

The dynamic equation of mass m_2 can be written as

$$m_2\ddot{u} + c\dot{u} + ku - c[N]\{\dot{q}\}_e - k[N]\{q\}_e = Q(t), \tag{37}$$

By combining (1) and (2), the dynamic system of equations of the cracked plate and mass m_2 are presented as follows:

$$\begin{gathered}\left([M_0]_e + \left[M_p^{m_1}\right]_e\right)\{\ddot{q}\}_e + \left[M_p^{m_2}\right]_e\ddot{u} + \left[C_p\right]_e\{\dot{q}\}_e + \left([K_c]_e + \left[K_p\right]_e\right)\{q\}_e = \{P\}_e \\ m_2\ddot{u} + c\dot{u} + ku - c[N]\{\dot{q}\}_e - k[N]\{q\}_e = Q(t),\end{gathered} \tag{38}$$

TABLE 1: The extreme value at the points A and B.

Case of load	w_A^{max} [cm]	$\ddot{w}_A^{max}$ [m/s^2]	σ_{intA}^{max} [N/m^2]	σ_{intB}^{max} [N/m^2]
MO	1.012	13.217	1.364×10^7	10.536×10^7
MM	1.122	42.4458	4.434x10^7	15.748x10^7

Or

$$\begin{bmatrix} [M_0]_e + [M_p^{m_1}]_e & [M_p^{m_2}]_e \\ [0] & m_2 \end{bmatrix} \begin{Bmatrix} \{\ddot{q}\}_e \\ \ddot{u} \end{Bmatrix} + \begin{bmatrix} [C_p]_e & [0] \\ -c[N] & c \end{bmatrix} \begin{Bmatrix} \{\dot{q}\}_e \\ \dot{u} \end{Bmatrix} + \begin{bmatrix} [K_c]_e + [K_p]_e & [0] \\ -k[N] & k \end{bmatrix} \begin{Bmatrix} \{q\}_e \\ u \end{Bmatrix} = \begin{Bmatrix} \{P\}_e \\ Q(t) \end{Bmatrix}. \quad (39)$$

2.2. Governing Differential Equations for Total System. By assembling all elements matrices and nodal force vectors, the governing equations of motions of the total system can be derived as

$$\begin{bmatrix} [M_0] + [M_p^{m_1}] & [M_p^{m_2}] \\ [0] & m_2 \end{bmatrix} \begin{Bmatrix} \{\ddot{q}\} \\ \ddot{u} \end{Bmatrix} + \begin{bmatrix} [C_p] + [C_R] & [0] \\ -c[N(\xi,\eta)] & c \end{bmatrix} \begin{Bmatrix} \{\dot{q}\} \\ \dot{u} \end{Bmatrix} + \begin{bmatrix} [K_0] + [K_c] + [K_p] & [0] \\ -k[N(\xi,\eta)] & k \end{bmatrix} \begin{Bmatrix} \{q\} \\ u \end{Bmatrix} = \begin{Bmatrix} \{P\} \\ Q(t) \end{Bmatrix}, \quad (40)$$

where $[M_0] = \sum_{N_0}[M_0]_e$ is the overall structural mass matrix, $[K_0] = \sum_{N_0-N_c}[K_0]_e$ is the overall structural stiffness matrix with total uncracked elements, $[K_c] = \sum_{N_c}[K_c]_e$ is the overall structural stiffness matrix with total cracked elements, $[M_p^{m_1}] = \sum_{Ne_{m1}}[M_p^{m_1}]_e$ is the overall mass matrix due to moving mass m_1, $[M_p^{m_2}] = \sum_{Ne_{m1}}[M_p^{m_2}]_e$ is the overall mass matrix due to moving mass m_2, $[C_p] = \sum_{Ne_{m1}}\sum[C_p]_e$ is the overall damping matrix due to moving mass m_1, and $[C_R] = \alpha_R[M_0] + \beta_R([K_0] + [K_c])$ is the overall structural damping matrix [14, 17].

This is a linear differential equation system with time dependence coefficient, which can be solved by using direct integration Newmark's method. A MATLAB program named Cracked_Plates_Moving_2019 was conducted to solve (40).

3. Numerical Analysis

We consider a rectangular cracked plate with size L = 3.0 m, W = 1.6 m, thickness h = 0.025 m, crack length W_{cr} = 0.5 m, and it appears in the middle of the plate (Figure 1). Material parameters of the plate: Young Modulus E = 2.0x10^{11} N/m^2, Poisson coefficient ν = 0.28, density ρ = 7800 kg/m^3. The boundary condition of the plate is SFSF (simply support, free/ simply support, free). The moving oscillator has mass m_1 = 300 kg connected with m_2 = 200 kg via spring with stiffness k = 1.5x10^5 N/m and damping element with resistance coefficient, c = 4.5x10^3 Ns/m, and k and c are parallel. Moving oscillator moves at velocity v = 10 m/s along the centerline y = W/2 of the plate.

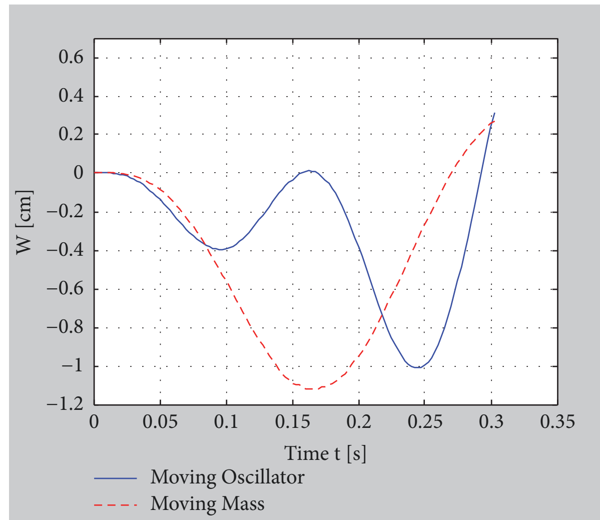

FIGURE 3: Dynamic vertical response at point A of the plate.

The results of the vibration of the plate subjected to moving oscillator (MO) and the effect of moving mass (MM) (M = m1 + m2 = 500 kg) are shown in Table 1 and Figures 3, 4, 5, and 6, in which the "int" symbol represents the intensity value (stress intensity and train intensity).

Comment: Compared to the case of cracked plate subjected to moving oscillator, the case of cracked plate subjected to moving mass indicates greater response of the plate. Therefore, the destructive capacity of the structure is greater.

3.1. The Effect of the Number of Cracks. To evaluate the effect of the number of cracks on vibration of cracked plate under moving oscillator, the three cases were investigated: Case 1: the plate has one crack in the middle (X = L/2, the basic problem); Case 2: the plate has one crack in the middle and one same size crack at X = L/4; Case 3: the plate has 3 cracks at X = L/4, L/2, 3L_p/4. The results of the vibration of the plate are shown in Table 2 and Figures 7, 8, 9, and 10.

Table 2: The extreme value at the points A and B.

Case	w_A^{max} [cm]	$\ddot{w}_A^{max}$ [m/s^2]	σ_{intA}^{max} [N/m^2]	σ_{intB}^{max} [N/m^2]
1	1.012	13.217	1.364x10^7	10.536×10^7
2	1.029	33.814	2.053x10^7	10.177×10^7
3	1.066	33.821	2.062x10^7	10.265×10^7

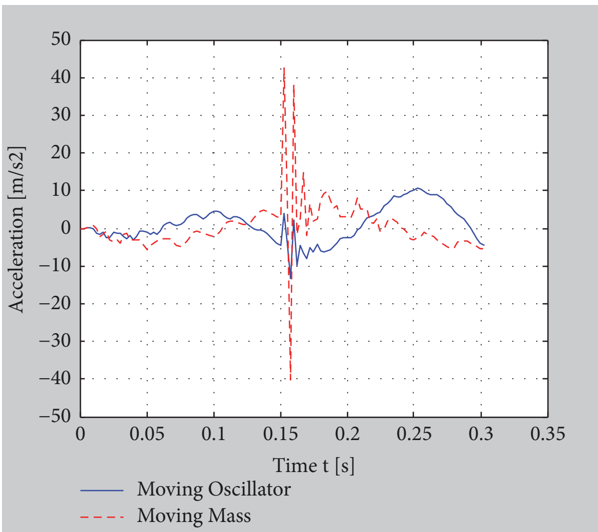

Figure 4: Vertical acceleration response at point A of the plate.

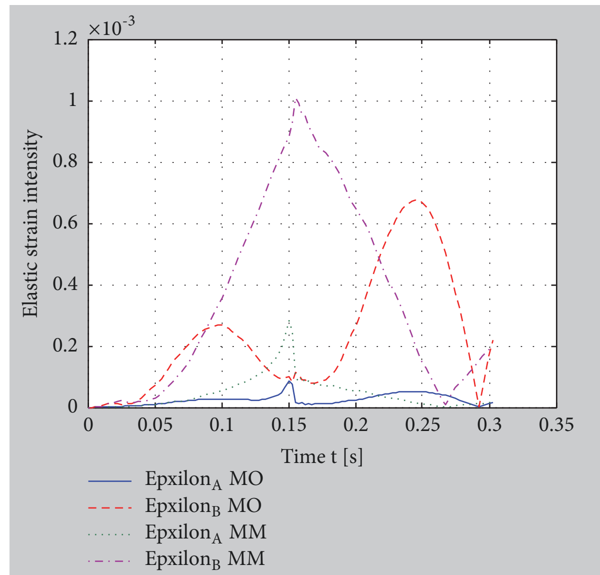

Figure 6: Strain response at points A and B of the plate.

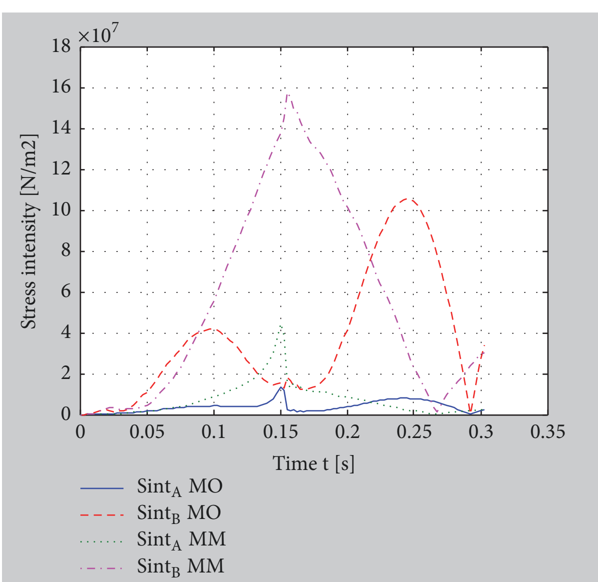

Figure 5: Stress response at points A and B of the plate.

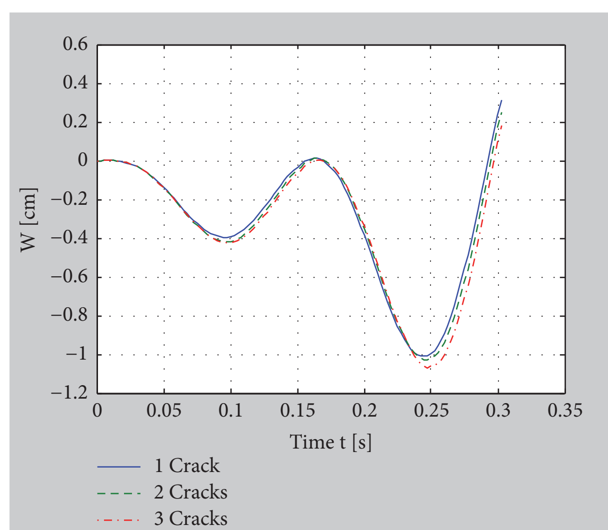

Figure 7: Dynamic vertical response at point A of the plate with different numbers of cracks.

Comment: Strain, displacement, stress, and acceleration at point A increase as the number of cracks increases, but these values fluctuate at the crack edge, sometimes increase and sometimes decrease.

3.2. The Effect of the Stiffness of the Spring k. To evaluate the effect of k hardness in the oscillation system on the response of the system, the authors examine the problem when k varies from 1x10^5 N/m to 9.0x10^5 N/m. Response of the system at

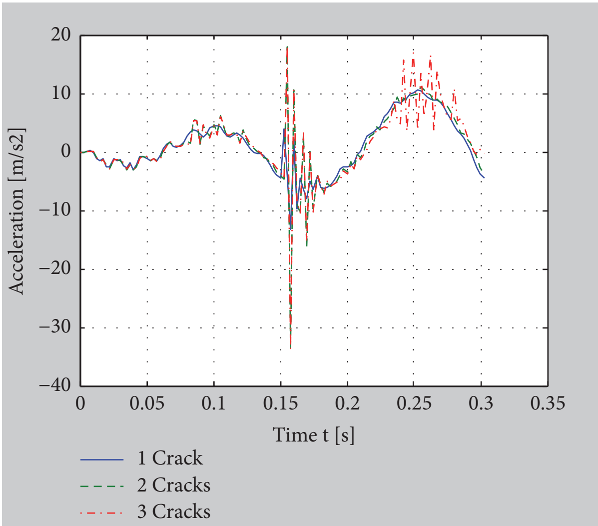

FIGURE 8: Vertical acceleration response at point A of the plate with different numbers of cracks.

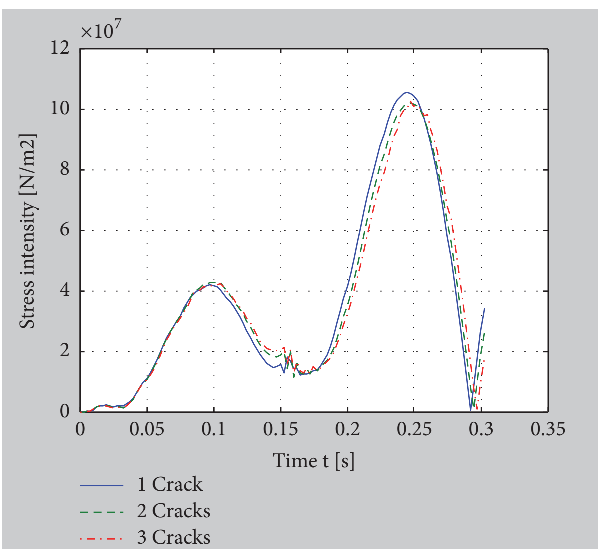

FIGURE 9: Stress response at point B of the plate with different numbers of cracks.

points A and B is shown in Table 3 and Figures 11, 12, 13, 14, 15, and 16.

Comment: When the k hardness changes, the oscillation of the system varies considerably. With the parameters of the given plate, the displacement response, acceleration, stress, and strain at the computed points are the greatest when k = $2.5x10^5$ N/m.

3.3. The Effect of Loading Velocity. The authors analyzed the dynamics of the plate with the speed of the oscillator system varying from 6 m/s to 14 m/s; the results are shown in Table 4 and Figures 17, 18, and 19.

Comment: When the speed of the oscillation system increases, the displacement and stress of the plate decrease,

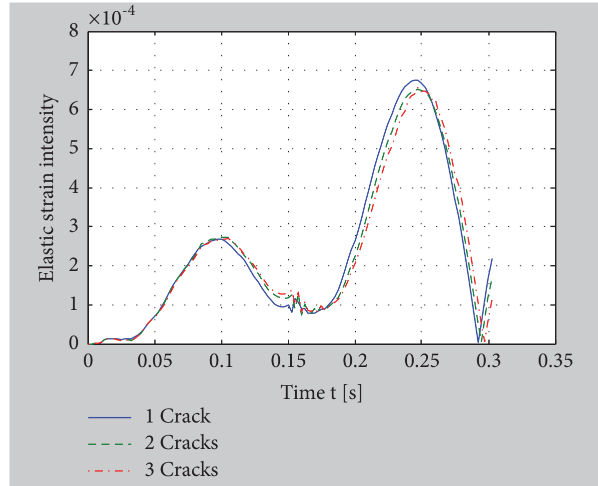

FIGURE 10: Strain response at point B of the plate with different numbers of cracks.

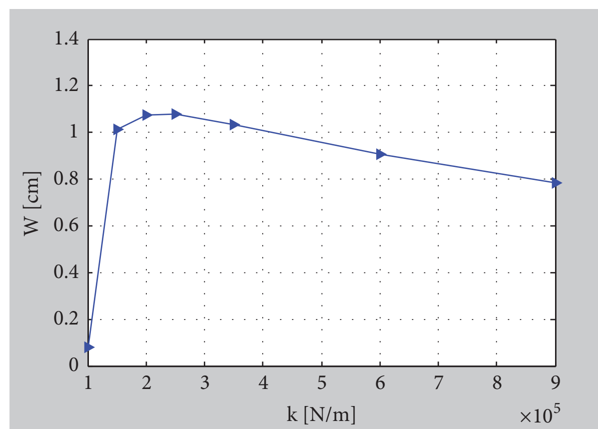

FIGURE 11: w_A^{max} - k relationship.

but there is no clear rule. According to the authors, the main reason may be due to the influence of the plate's free vibration frequency and the moving oscillator; this is the difference with the case of the plate subjected to moving mass.

4. Conclusions

In the end, with the set of survey parameters, the case of the cracked plate under the moving mass is more dangerous than the case of moving oscillators operates. However, the problem of texture affected by the oscillation system is complex. In each case, a reevaluation is needed. The response of the system depends on the interrelation between the frequency of the stimulus and the natural frequency of the system.

The results show that stress and strain at the crack head are much larger than they are at other sites. These values vary considerably when the number of cracks and k hardness are changed.

Table 3: The extreme value at the points A and B.

$k\times10^5$ [N/m]	w_A^{max} [cm]	$\ddot{w}_A^{max}$ [m/s^2]	σ_{intA}^{max} [N/m^2]	σ_{intB}^{max} [N/m^2]
1.0	0.081	8.942	0.813×10^7	8.426×10^7
1.5	1.012	13.217	1.364×10^7	10.536×10^7
2.0	1.075	19.415	2.285×10^7	11.284×10^7
2.5	1.078	23.073	3.150×10^7	11.553×10^7
3.5	1.033	21.224	4.036×10^7	11.363×10^7
6.0	0.905	17.740	2.380×10^7	11.213×10^7
9.0	0.783	12.360	1.554×10^7	8.693×10^7

Table 4: The extreme value at the points A and B.

v [m/s]	w_A^{max} [cm]	$\ddot{w}_A^{max}$ [m/s^2]	σ_{intA}^{max} [N/m^2]	σ_{intB}^{max} [N/m^2]
6	1.211	15.429	4.352×10^7	16.323×10^7
8	1.210	13.816	2.931×10^7	13.124×10^7
10	1.012	13.217	1.364×10^7	10.536×10^7
12	0.724	10.201	0.970×10^7	7.718×10^7
14	0.537	11.897	1.137×10^7	6.048×10^7

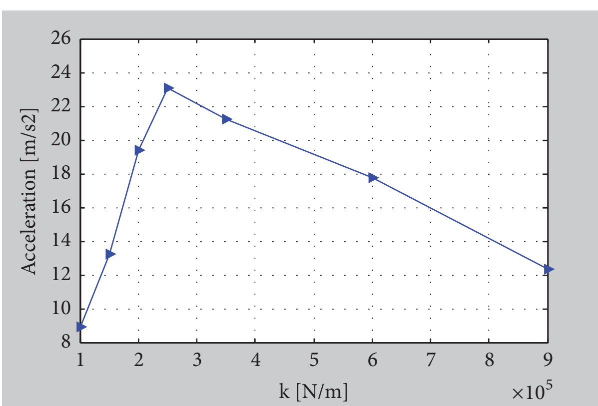

Figure 12: $\ddot{w}_A^{max}$ - k relationship.

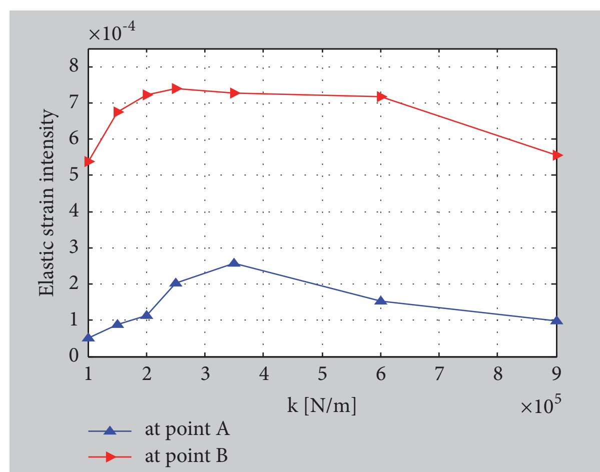

Figure 14: ε_{intA}^{max} and ε_{intB}^{max} - k relationship.

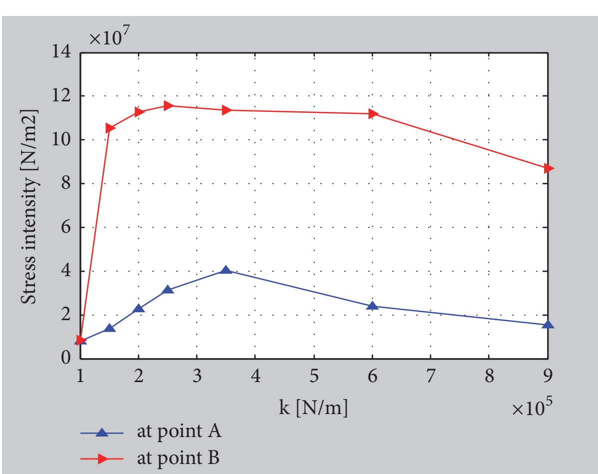

Figure 13: σ_{intA}^{max} and σ_{intB}^{max} - k relationship.

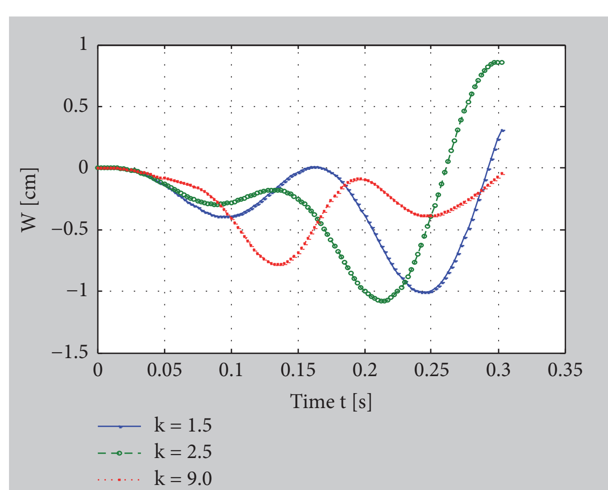

Figure 15: Stress response at point A of the plate with different k.

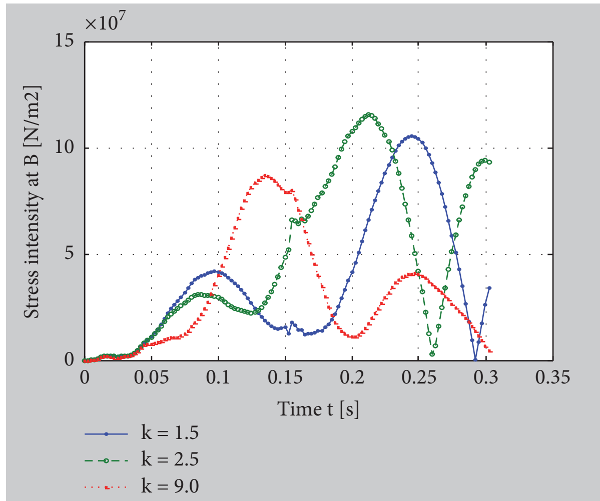

FIGURE 16: Stress response at point B of the plate with different k.

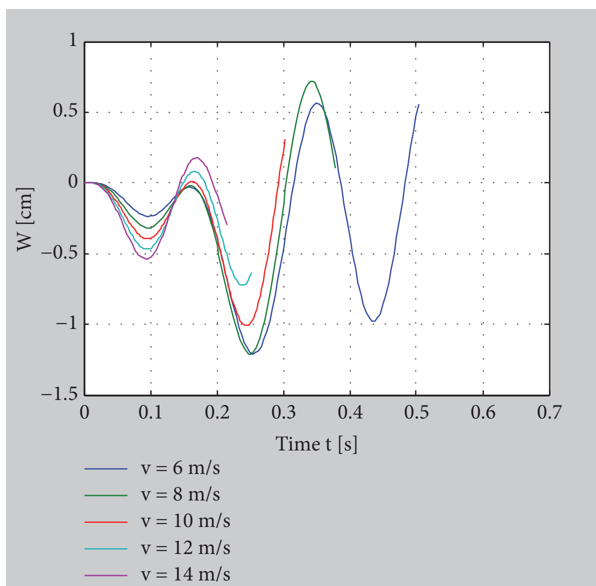

FIGURE 17: Vertical displacement response at point A of the plate with different v.

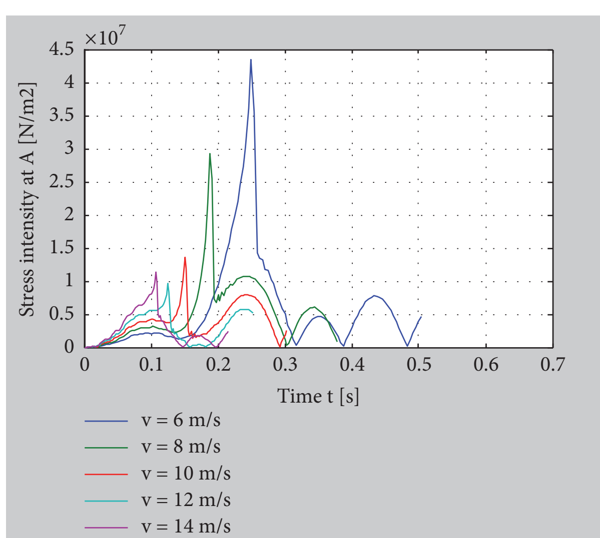

FIGURE 18: Stress response at point A of the plate with different v.

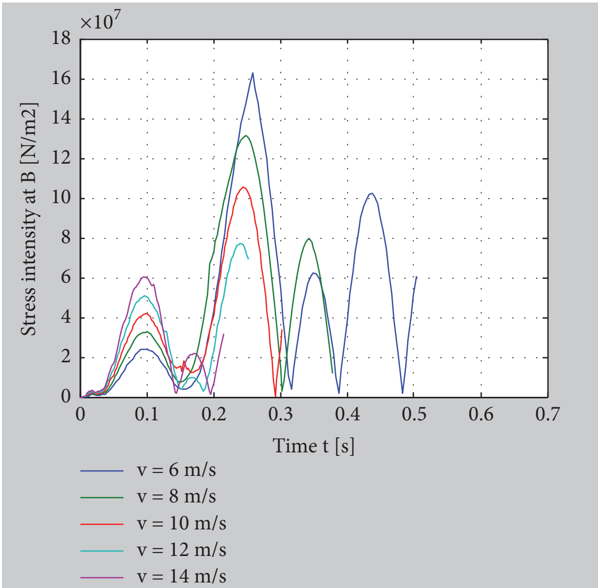

FIGURE 19: Stress response at point B of the plate with different v.

Appendix

A.

The transformation matrix $[T]$ is

$$[T] = \begin{bmatrix} 0 & \frac{2}{H} & 0 & 0 & 0 & 0 & 0 & -\frac{2}{L} & -1 \\ 1 & 1 & 0 & 0 & 0 & 0 & 0 & 0 & 0 \\ 0 & 0 & 0 & 0 & 0 & 0 & -1 & 1 & 0 \\ 0 & -\frac{2}{H} & 0 & \frac{2}{L} & 0 & 0 & 0 & 0 & 1 \\ -1 & 1 & 0 & 0 & 0 & 0 & 0 & 0 & 0 \\ 0 & 0 & -1 & -1 & 0 & 0 & 0 & 0 & 0 \\ 0 & 0 & 0 & -\frac{2}{L} & 0 & \frac{2}{H} & 0 & 0 & -1 \\ 0 & 0 & 0 & 0 & -1 & -1 & 0 & 0 & 0 \\ 0 & 0 & 1 & -1 & 0 & 0 & 0 & 0 & 0 \\ 0 & 0 & 0 & 0 & 0 & -\frac{2}{H} & 0 & \frac{2}{L} & 1 \\ 0 & 0 & 0 & 0 & 0 & -1 & 0 & 0 & 0 \\ 0 & 0 & 0 & 0 & 0 & 0 & 1 & 1 & 0 \end{bmatrix}, \quad \text{(A.1)}$$

B.

The flexibility matrix of the noncracked element $[C_0^f]$ is

$$[C_0^f] = \frac{12}{Eh^3} \begin{bmatrix} \frac{4W}{L} & & & & & & & & \\ 0 & \frac{4W}{3L} & & & & & & & \\ -\nu & \nu & \frac{4L}{W} & & & & sym & & \\ -\nu & \nu & 0 & \frac{4L}{3W} & & & & & \\ -\frac{2W}{L} & 0 & -\nu & -\nu & \frac{4W}{L} & & & & \\ 0 & \frac{2W}{3L} & -\nu & \nu & 0 & \frac{4W}{3L} & & & \\ -\nu & \nu & -\frac{2L}{W} & 0 & -\nu & \nu & \frac{4L}{W} & & \\ -\nu & \nu & 0 & \frac{2L}{3W} & -\nu & \nu & 0 & \frac{4L}{3W} & \\ 0 & 0 & 0 & 0 & 0 & 0 & 0 & 0 & 2(1+\nu)LW \end{bmatrix}, \quad \text{(B.1)}$$

C.

The flexibility matrix due to the presence of the crack $[C_1^f]$ is

(i) Crack parallel to the x-axis of the element:

$$[C_1^f] = \frac{6}{Eh^3} \begin{bmatrix} c_{11} & & & & & & & & \\ 0 & 0 & & & & & & & \\ 0 & 0 & 0 & & & sym & & & \\ 0 & 0 & 0 & 0 & & & & & \\ c_{51} & 0 & 0 & 0 & c_{55} & & & & \\ 0 & 0 & 0 & 0 & 0 & 0 & & & \\ 0 & 0 & 0 & 0 & 0 & 0 & 0 & & \\ 0 & 0 & 0 & 0 & 0 & 0 & 0 & 0 & \\ 0 & 0 & 0 & 0 & 0 & 0 & 0 & 0 & c_{99} \end{bmatrix}, \quad \text{(C.1)}$$

(ii) Crack parallel to the y-axis of the element:

$$[C_1^f] = \frac{6}{Eh^3} \begin{bmatrix} 0 & & & & & & & & \\ 0 & 0 & & & & & & & \\ 0 & 0 & c_{33} & & sym & & & & \\ 0 & 0 & 0 & 0 & & & & & \\ 0 & 0 & 0 & 0 & 0 & & & & \\ 0 & 0 & 0 & 0 & 0 & 0 & & & \\ 0 & 0 & c_{73} & 0 & 0 & 0 & c_{77} & & \\ 0 & 0 & 0 & 0 & 0 & 0 & 0 & 0 & \\ 0 & 0 & 0 & 0 & 0 & 0 & 0 & 0 & c_{99} \end{bmatrix}, \quad \text{(C.2)}$$

where

$$
\begin{aligned}
c_{11} &= 4\Pi\Phi_1^2 \int_{-\bar{a}}^{\bar{a}} \bar{a}\,(2-0.75\bar{a})^2 f^2(\bar{a})\,d\bar{a},\\
c_{33} &= 4\Pi\Phi_1^2 \int_{-\bar{a}}^{\bar{a}} \bar{a}\,(-1+0.75\bar{a})^2 f^2(\bar{a})\,d\bar{a},\\
c_{55} &= 4\Pi\Phi_1^2 \int_{-\bar{a}}^{\bar{a}} \bar{a}\,(-1+0.75\bar{a})^2 f^2(\bar{a})\,d\bar{a},\\
c_{77} &= 4\Pi\Phi_1^2 \int_{-\bar{a}}^{\bar{a}} \bar{a}\,(2-0.75\bar{a})^2 f^2(\bar{a})\,d\bar{a},\\
c_{99} &= \Pi W^2\Phi_2^2 \int_{-\bar{a}}^{\bar{a}} \bar{a} f^2(\bar{a})\,d\bar{a},\\
c_{51} &= 2\Pi\Phi_1^2 \int_{-\bar{a}}^{\bar{a}} \bar{a}\,(2-0.75\bar{a})(-1+0.75\bar{a}) f^2(\bar{a})\,d\bar{a},\\
c_{73} &= 2\Pi\Phi_1^2 \int_{-\bar{a}}^{\bar{a}} \bar{a}\,(-1+0.75\bar{a})(2-0.75\bar{a}) f^2(\bar{a})\,d\bar{a},\\
f(\bar{a}) &= 1.0 + 0.01876\bar{a} + 0.1825\bar{a}^2 + 2.024\bar{a}^3 - 2.4316\bar{a}^4,
\end{aligned} \tag{C.3}
$$

with $\bar{a} = W_{cr}/L$ when the crack is parallel to the x-axis, and $\bar{a} = W_{cr}/W$ when the crack is parallel to the y-axis of the element, and Φ_i (i=1,2) are correction functions given in [8].

Data Availability

The data used to support the findings of this study are available from the corresponding author upon request.

Conflicts of Interest

The authors declare that there are no conflicts of interest regarding the publication of this paper.

Acknowledgments

This research was supported by Le Quy Don University.

References

[1] N. T. Chung and L. P. Binh, "Nonlinear dynamic analysis of cracked beam on elastic foundation subjected to moving mass," *International Journal of Advanced Engineering Research and Science*, vol. 4, no. 9, pp. 73–81, 2017.

[2] S. R. Mohebpour, P. Malekzadeh, and A. A. Ahmadzadeh, "Dynamic analysis of laminated composite plates subjected to a moving oscillator by FEM," *Composite Structures*, vol. 93, no. 6, pp. 1574–1583, 2011.

[3] P. Malekzadeh, A. Fiouz, and H. Razi, "Three-dimensional dynamic analysis of laminated composite plates subjected to moving load," *Composite Structures*, vol. 90, no. 2, pp. 105–114, 2009.

[4] Q. Song, Z. Liu, J. Shi, and Y. Wan, "Parametric study of dynamic response of sandwich plate under moving loads," *Thin-Walled Structures*, vol. 123, pp. 82–99, 2018.

[5] Q. Song, J. Shi, and Z. Liu, "Vibration analysis of functionally graded plate with a moving mass," *Applied Mathematical Modelling*, vol. 46, pp. 141–160, 2017.

[6] A. Mamandi, R. Mohsenzadeh, and M. H. Kargarnovin, "Nonlinear dynamic analysis of a rectangular plate subjected to accelerated/decelerated moving load," *Journal of Theoretical and Applied Mechanics*, vol. 53, no. 1, pp. 151–166, 2015.

[7] A. Vosoughi, P. Malekzadeh, and H. Razi, "Response of moderately thick laminated composite plates on elastic foundation subjected to moving load," *Composite Structures*, vol. 97, pp. 286–295, 2013.

[8] Q. Guan-Liang, G. Song-Nian, and J. Jie-Sheng, "A finite element model of cracked plates application to vibration problems," *Computers & Structures*, vol. 39, no. 5, pp. 483–487, 1991.

[9] M. Krawczuk and W. M. Ostachowicz, "A finite plate element for dynamic analysis of a cracked plate," *Computer Methods Applied Mechanics and Engineering*, vol. 115, no. 1-2, pp. 67–78, 1994.

[10] T. Yin and H. Lam, "Dynamic analysis of finite-length circular cylindrical shells with a circumferential surface crack," *Journal of Engineering Mechanics*, vol. 139, no. 10, pp. 1419–1434, 2013.

[11] H. Serdar, *Vibration Analysis of Systems Subjected to Moving Loads by Using Finite Element Method [A Thesis]*, Graduate School of Natural and Applied Sciences, 2005.

[12] D. H. Li, X. Yang, R. L. Qian, and D. Xu, "Static and dynamic response analysis of functionally graded material plates with damage," *Mechanics of Advanced Materials and Structures*, pp. 1–14, 2018.

[13] F. Ladislav, *Vibration of Solid and Structures under Moving Loads*, Thomas Telford, 1999.

[14] K. J. Bathe and E. L. Wilson, *Numerical Method in Finite Method Analysis Prentice*, Hall of India Private Limited, New Delhi, India, 1978.

[15] J. N. Reddy, *Mechanics of Laminated Composite Plates and Shells: Theory and Analysis*, CRC Press, 2004.

[16] J. S. Przemieniecki, *Theory of Matrix Structural Analysis*, McGraw-Hill, New York, NY, USA, 1968.

[17] J. P. Wolf, *Dynamic Soil-Structure Interaction Analysis in Time domain*, vol. 07632, Prentice-Hall Inc., Englewood Cliffs, NJ, USA, 1988.

[18] S. E. Khadem and M. Rezaee, "Introduction of modified comparison functions for vibration analysis of a rectangular cracked plate," *Journal of Sound and Vibration*, vol. 236, no. 2, pp. 245–258, 2000.